Bearing Capacity Factors of Ring Footings

Ehsan Seyedi Hosseininia

Iranian Journal of Science and Technology, Transactions of Civil Engineering

ISSN 2228-6160
Volume 40
Number 2

Iran. J. Sci. Technol.Trans. Civ. Eng.
(2016) 40:121-132
DOI 10.1007/s40996-016-0003-6

Springer

Iran. J. Sci. Technol.Trans. Civ. Eng. (2016) 40:121–132
DOI 10.1007/s40996-016-0003-6

RESEARCH PAPER

Bearing Capacity Factors of Ring Footings

Ehsan Seyedi Hosseininia[1]

Received: 14 May 2014 / Accepted: 20 May 2015 / Published online: 21 April 2016

Abstract In the present paper, bearing capacity factors were determined for ring footings. The footing roughness is considered in the analyses including smooth and a perfectly rough footing base. The computations were achieved by numerical simulation of ring footings using the finite difference method for different inner to outer ring radii ratio. Based on the results, it is shown that the value of all three bearing capacity factors, i.e., N_γ^*, N_q^*, and N_c^* reduces with the increase in inner to outer ring radii ratio. The reduction effect is more sensible for N_γ^* factor. Furthermore, it is seen that the footing roughness augments the value of the three bearing capacity factors. The results of the present work for N_γ^* were compared with those of the previous published data including experimental and numerical studies, which reveals acceptable agreements. The obtained values of factors were compared for the case of circular footings as a benchmark in the analyses, which are in accordance with the previously published data. In the end, by applying some examples, it was shown that using the proposed bearing capacity equation, which is based on the superposition of different plastic conditions, is conservative and safe with respect to complete plastic analysis.

Keywords Numerical modeling · Ring footings · Bearing capacity factors · Frictional–cohesive soils

✉ Ehsan Seyedi Hosseininia
eseyedi@um.ac.ir

[1] Department of Civil Engineering, Faculty of Engineering, Ferdowsi University of Mashhad, Mashhad, Islamic Republic of Iran

1 Introduction

Due to the symmetrical geometry of structures such as silos, storage tank, chimneys, and cooling towers, ring footings are appropriate since the amount of materials is more economical in comparison with circular footings. In order to have safe and economical design of such footings, good knowledge about the bearing capacity of such footings is required.

The bearing capacity of footings is calculated by virtue of three N_c, N_q, and N_γ bearing capacity factors appearing in sets of bearing capacity equations similar to the well-known Terzaghi's classical equation, which is the superposition of these factors (e.g., Meyerhof 1951; Terzaghi 1943; Vesic 1973). Nowadays, apart from simple cases of footings, diverse analytical and numerical methods have been used to study more complicated problems of footing bearing capacities (e.g., Haghbin and Ghazavi 2013; Keshavarz et al. 2011; Majidi and Mirghasemi 2008; Rostami and Ghazavi 2015).

Searching the literature for the bearing capacity factors of ring footings, there have been few attempts to investigate the value of N_γ and the other two factors are ignored. The researches indicate that the bearing capacity is influenced by the ring shape, which is generally explained by the inner to outer ring radii ratio. By using the method of characteristics, Kumar and Gosh (2005) obtained the N_γ for both smooth and rough ring footing bases for high range of soil friction angle ($\phi = 5$–$50°$). They found that the N_γ factor, whose value is bigger for rough surface against smooth surface, generally decreases continuously with an increase in ring radii ratio for both cases. Zhao and Wang (2008) used the finite difference method to compute N_γ for low soil frictions ($\phi = 5$–$30°$) for smooth and perfectly rough footing bases. More recently, by using the finite

difference method, Benmebarek et al. (2012) examined numerically the effect of associativity and nonassociativity of the soil for $\phi = 20$–$45°$ on the N_γ of ring footings. They concluded that soil dilation angle has a major influence on the value of N_γ when the soil displays high nonassociativity for $\phi > 30°$. By assuming associative behavior for the soil, they compared their results with those of previously mentioned works, which were based on finite element method or method of characteristics. Their obtained value of N_γ has good agreement with the case of smooth footing, but there are some discrepancies for the case of the rough footing. In the latter case, the obtained values of N_γ are calculated larger for the radii ratio smaller than 0.33 while the N_γ of the footings with the radii ratio bigger than 0.33 were calculated smaller.

There are a few experimental investigations on the bearing capacity of ring footings on cohesionless soils in the literature review (Boushehrian and Hataf 2003; Clark 1998; Ohri et al. 1997; Hataf and Razavi 2003). In contrast to the numerical methods, these laboratorial researches indicate that the bearing capacity does not decrease continuously with the increase in the radii ratio, but a maximum bearing capacity is often reachable at about the radii ratio of 0.2–0.4. It is generally believed that this occurrence is related to the arching effect inside the whole of the ring footing.

The aim of the present work is to determine all three bearing capacity factors for ring footings by means of the finite difference method. Although N_γ has been investigated in previous studies, there are no data about the other two factors N_q and N_c. These factors are defined in the form of traditional Terzaghi's bearing capacity equation, which uses the superposition of the effect of unit weight, surcharge, and the soil cohesion. In addition, the roughness of the footing base is also taken into account. Attempts are also made to derive mathematical expressions of the bearing capacity factors in order to have practical formulas for estimating the bearing capacity of ring footings. In the end, the conservativeness of the superposition applied in the bearing capacity equation is evaluated by considering several examples.

2 Problem Definition

In this study, the geometry of a ring footing is defined by inner and outer radii $(r_\mathrm{i}, r_\mathrm{o})$, respectively, which rests on a frictional–cohesive soil with a horizontal ground surface. The geometry can be alternatively defined by the radii ratio $n = r_\mathrm{i}/r_\mathrm{o}$. The footing is to support only vertical load whose point of application coincides with the center of the ring footing. The ground surface besides the footing is loaded with a uniform normal surcharge pressure (q_0) without any shear stress. In the case of smooth footing base, it is assumed that there is no shear stress mobilized over the base, while a rough footing base has a perfect bonding with the ground underneath.

Now, consider that a ring footing with an outer diameter $D_\mathrm{o} = 2r_0$ rests over the ground, where a uniform surcharge (q_0) is applied. The ultimate bearing capacity (q_{ult}) of a ring footing is expressed in a similar form of the Terzaghi's bearing capacity equation as follows:

$$q_{ult} = cN_c^* + q_0 N_q^* + 0.5\gamma D_o N_\gamma^* \tag{1}$$

where γ and c are the unit weight and cohesion of the soil. The terms N_c^*, N_q^*, and N_γ^* are bearing capacity factors of the ring footing, which take into account individually the effect of soil cohesion, surcharge, and unit weight, respectively. In addition, the effect of footing shape, i.e., the ring radii ratio, n, is implicitly taken into consideration.

Based on Eq. (1) introduced above, the bearing capacity factors can be obtained by considering three simplified problems. To find the factor N_γ^*, it is sufficient to consider a problem in which the soil is cohesionless $(c = 0)$ and no surcharge exists on the ground surface $(q_0 = 0)$. In such case, the equation reduces to $q_\mathrm{ult} = 0.5\gamma D_\mathrm{o} N_\gamma^* = r_\mathrm{o}\gamma N_\gamma^*$ and hence, $N_\gamma^* = q_\mathrm{ult}/r_\mathrm{o}\gamma$. In order to calculate the factor N_q^*, it is supposed that the soil has neither unit weight nor cohesion, i.e., $\gamma = 0$, $c = 0$. Instead, there is a uniform surcharge (q_0) over the ground surface, which represents the weight of overburden beside the footing at the base level. Hence, the simplification results in $N_q^* = q_\mathrm{ult}/q_0$. Finally, the factor N_c^* can be assessed simply by taking the soil as weightless $(\gamma = 0)$, but cohesive without any surcharge $(q_0 = 0)$ on the ground surface. Thus, the calculation gives $N_c^* = q_\mathrm{ult}/c$.

3 Numerical Modeling and Bearing Capacity Factors Determination

The analysis in the present work has been carried out using the FLAC computer code, which is a finite difference explicit program. The computations have been done for four cases including circular $(n = 0)$ and ring footings with the radii ratio $n = 0.25$, 0.5, and 0.75 with the outer radius $r_0 = 1$ m. Figure 1 presents the global model schematics used in the simulations. Due to the simple geometry of the ring footing, an axisymmetric modeling is considered here. According to Fig. 1a, the vertical boundaries of the model are restricted to be moved only in the horizontal direction, while the lower boundary condition is fixed in both directions. The load from the footing as well as surcharge (if existed) is applied to the upper boundary of the model. The footing load is applied by using a downward velocity

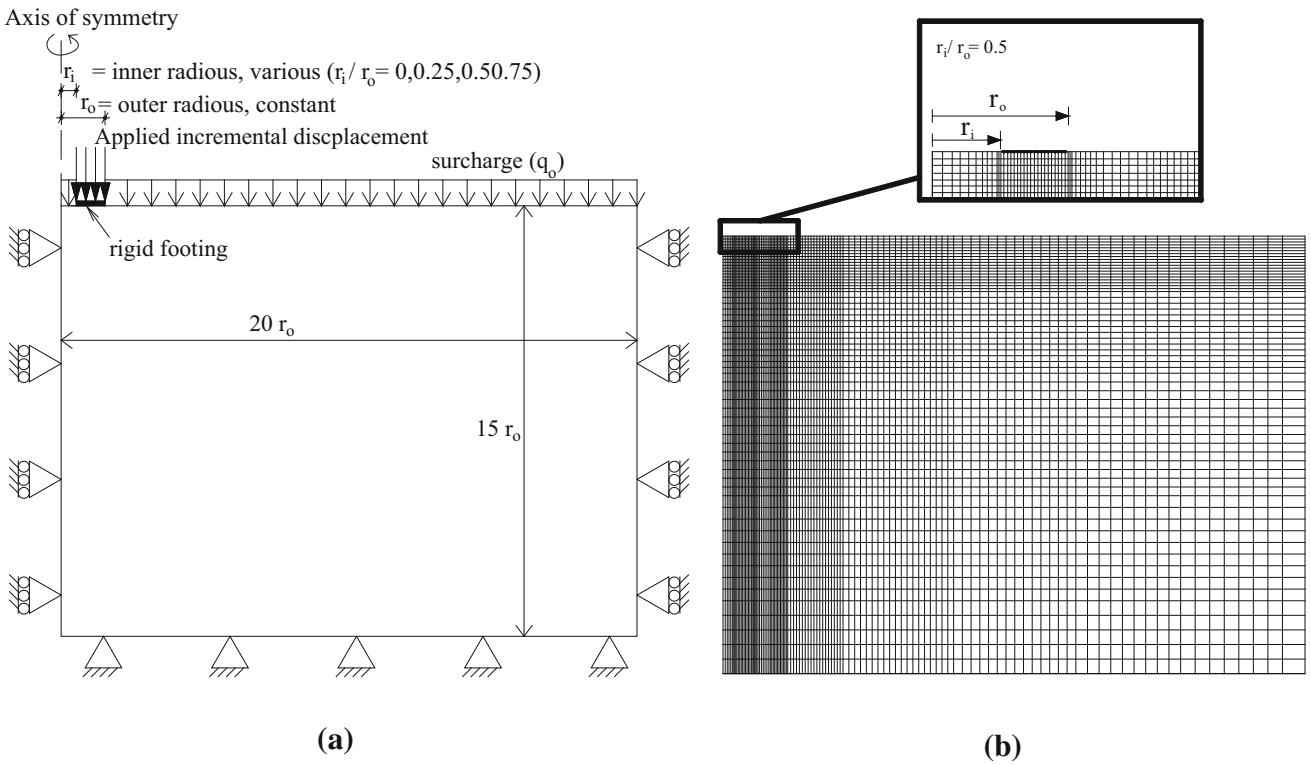

Fig. 1 Schematics of the numerical model for ring footing: **a** dimension and boundary conditions; **b** grid used in the simulations for $n = 0.5$

with a small time increment at the location of the ring footing area. The model dimensions were chosen to be $20r_o$ and $15r_o$ in the horizontal and vertical directions, respectively, in order to minimize boundary effect. The model dimension was adopted by checking that the plastic regions generated in the soil do not reach the boundaries. The grid size is considered to be increased by getting distance from the edges to the sides of the model. For each case of ring radii ratio (n), an individual mesh has been generated. The numerical mesh used in the simulation for $n = 0.5$ is depicted in Fig. 1b. It is also noted that for checking the grid size, a more refined mesh (about twice) for $n = 0.5$ has been also taken into consideration in the numerical simulations. However, since the results of these series were very close to those of the present mesh and due to the time saving, the global theme of the presented mesh (Fig. 1b) was used for the rest of the ring footings.

The modeling procedure of a bearing capacity problem follows two stages including the allocation of geostatic stress to the soil grid followed by applying the load from the ring footing. In the first stage, the stresses inside the soil grid are introduced and the model is brought into equilibrium by running some calculation steps. In the case of N_γ^* problem, a linear distribution of geostatic stress $(= \gamma z)$ with depth (z) is required to be defined. In the case of N_q^* calculation, since the soil is weightless and instead, the soil surface experiences a uniform pressure, the geostatic stress in the soil is introduced as a constant magnitude equal to the ground surface pressure (q_0). Finally, in the case of N_c^* calculation, since the soil is weightless and there is no surcharge over the ground surface, no geostatic stress is needed to be defined in the soil grid. The second stage of numerical modeling concerns the implantation of the ring footing load over the ground surface. The footing load is applied by using a downward velocity over the grid points representing the footing area. A trial and error process has been performed to reach a correct modeling of the bearing capacity problem. For the first estimation, a velocity of 10^{-6} m/step was applied to the footing area until a steady plastic flow is achieved such that a constant pressure at the footing base is realized. In the next step, a new analysis is re-performed by using a reduced (half) velocity. This procedure, especially for high values of soil friction angles, has been repeated until the difference between the bearing capacity values computed at two successive steady plastic flow states became negligible.

In the case of smooth footing base, the grid points representing the footing base are left free to move in the radial direction, while a rough footing is simulated by fixing the displacement in the radial direction.

Since the footing is rigid, the average pressure (q_{ave}) is defined as the summation of the vertical component of applied load of the grid points at the footing base divided by the footing base area, as follows:

$$q_{ave} = \frac{2\pi \sum_j F_y^j r^j}{\pi\left(r_o^2 - r_i^2\right)} \quad (2)$$

where F_y^j and r^j are the nodal reaction force in the vertical direction and the associated radius of the jth grid point at the footing base in the numerical modeling.

In the analyses of the present work, the elastic-perfectly plastic Mohr–Coulomb model is used for the soil material. The soil parameters are unit weight $\gamma = 20$ kN/m^3, shear modulus $G = 10$ MPa, bulk modulus $K = 20$ MPa, and a series of soil friction angle $\phi = 0$–$45°$ with intervals of five degrees. It is assumed that the soil behaves in an associative manner; i.e., the angle of soil dilation (ψ) is equal to the soil friction angle. This assumption was made in order to verify and evaluate the results of the present study with those of other published data in which, the soil behavior has been mostly considered as associative. In the calculation of N_q^*, a uniform surcharge $q_0 = 100$ kPa is considered over the ground surface in the modeling process. Regarding the calculation of N_c^*, the soil cohesion is considered to be $c = 100$ kPa.

4 Results and Comparisons

Based on the numerical procedure described above, the three bearing capacity factors are calculated from the applied pressure (q_{ave}) on the footings. Analyses are categorized into three groups corresponding to the factors. Figure 2 presents examples of two groups including N_γ and N_q problems (for $\phi = 20, 35°$) for circular and ring footings (with $n = 0.5$) in terms of the variation of applied pressure with regard to the settlement. In order to calculate the corresponding factor, the ultimate value is taken into consideration.

Figure 3 presents the plastic zones generated in the soil below the circular and ring footings ($n = 0.5$) for N_γ and N_q problems. These snapshots correspond to the last part of the load–settlement curves shown in Fig. 2 where the footings cannot tolerate extra pressure accompanied by large displacements. According to Fig. 3, the extent of plastic zones is larger for N_q problems with respect to N_γ problems. In addition, the plastic zone is further extended for larger value of internal friction angle.

The variations of the factors $(N_\gamma^*, N_q^*, N_c^*)$ with ring radii ratio (n) are depicted in graphical form in a semilogarithmical coordinate system as shown in Fig. 4. It can be seen that the ring radii ratio has a decreasing effect on the value of factors. The variation of N_γ^* is more than that of N_q^* and N_c^* factors. Furthermore, it can be understood that the footing roughness increases the value of the factors. Among them, the growth in the value of N_γ^* has been intensified more by the footing roughness. The same result has been reported by others for the case of circular footings (e.g., Houlsby 1982; Kumar and Khatri 2011).

4.1 Bearing Capacity Factor N_γ^*

To evaluate the results obtained from the analyses, N_γ^* of ring footings from Kumar and Gosh (2005) and other FLAC results (Zhao and Wang 2008; Benmebarek et al. 2012) are presented separately for smooth and rough footings in Table 1. N_γ^* of the present work are slightly greater than those from the method of characteristics as well as those analyses by others using FDM. The inconsistency between the analytical methods originates from the dissimilarity of calculation approaches such that FLAC performs stress–strain analysis, but only stress components play the role in the analysis with the method of characteristics. The dissimilarity between the results of analyses by FDM may exist in the difference in the size of grids, the model dimension, and boundary conditions.

In order to verify the numerical simulations of this work, the results are compared with those of a series of physical tests using centrifuge modeling technique reported by Clark (Clark 1998). These tests are more valuable than small scale tests because experimental tests

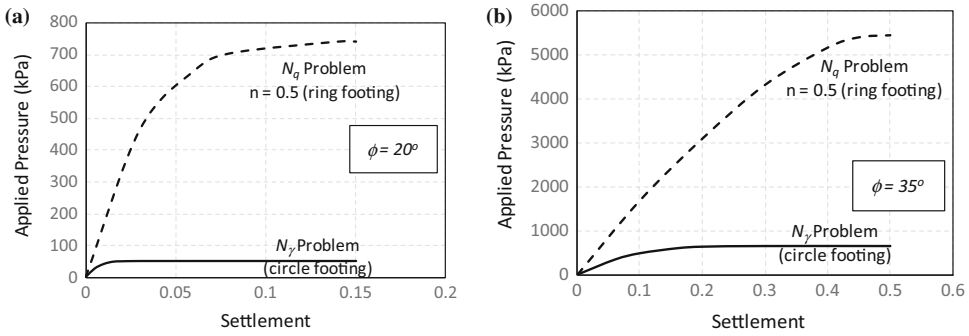

Fig. 2 Variation of applied pressure versus settlement of footings in N_γ and N_q problems, **a** $\phi = 20°$; **b** $\phi = 35°$

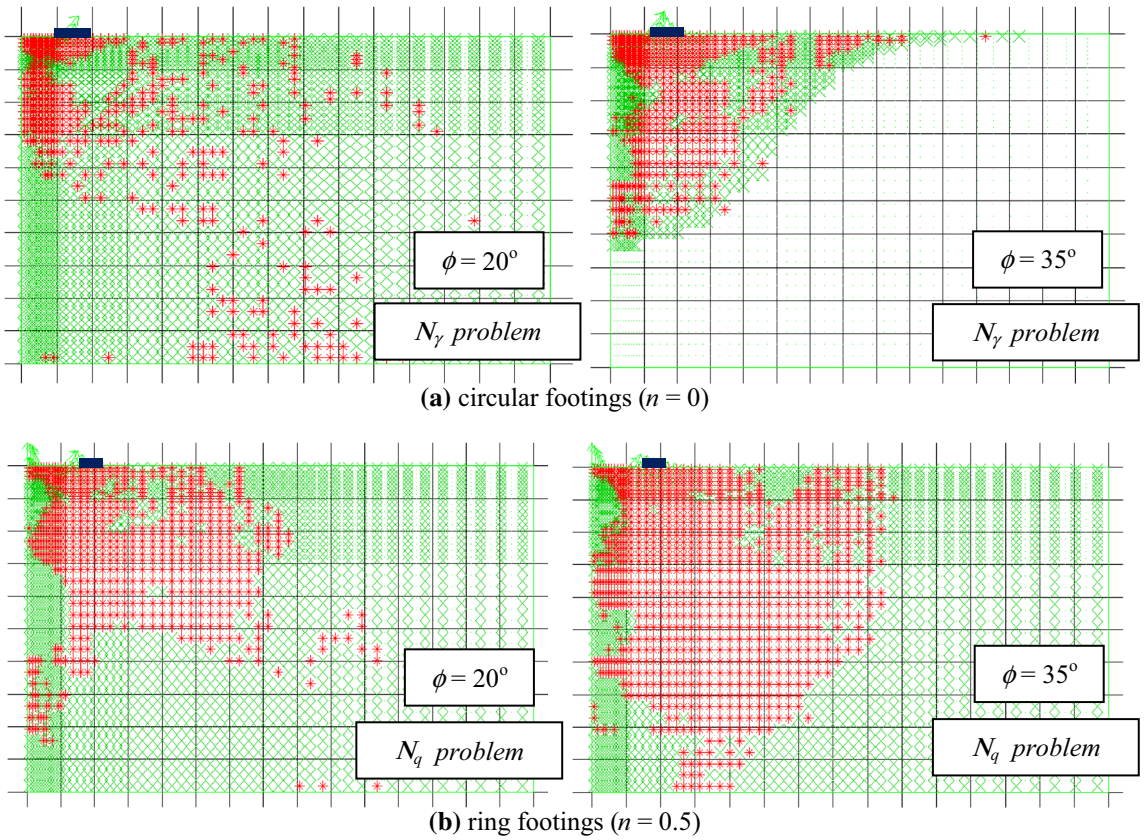

Fig. 3 Presentation of plastic zones in the soil below the footings: **a** circular footings ($n = 0$). **b** Ring footings with $n = 0.5$. *Red points* indicate plastic points

(De Beer 1965) and centrifuge tests (Clark 1998; Taylor 1995; Zhu et al. 1996) showed that footing size has effect on N_γ^*. In the centrifuge tests by Clark (1998), a series of reduced-scale square and circular ring footings were tested. Five ring footing models with radii ratio (n) of zero, 0.3, 0.45, 0.6, and 0.8 were tested at high acceleration level of 100 g to simulate the behavior of large-scale prototype square footings with an outside width of 4 m. These footings were equivalent to circular ring footings with the outer diameter of 4.5 m. The footings were rigid with a rough surface. The loading over the footings was applied, and the peak pressure was considered as the bearing capacity of the footing. The tests were carried out over the dense silica sand with the density index of 88 %. Triaxial compression tests were performed over the dense silica sand with a wide range of confining pressure from 25 to 2500 kPa, and the peak internal friction angles were measured. According to the laboratory test results, there is a linear relationship between the peak friction angle and the logarithm of the confining pressure. According to the back calculations presented in "Appendix 1," the peak soil friction angle mobilized under the footing is estimated as 39.5–41.5°.

Figure 5 presents the variation of back calculated values of N_γ^* from experiment as well as those from different analyses versus the ring radii ratio (n) with the assumption of $\phi = 40°$. According to the centrifuge tests, the bearing capacity initially increased about 10 % when the radii ratio increased from zero to about 0.3. With further increase in radii ratio, the bearing capacity decreases. The same regime was also found in the small scale test performed by Boushehrian and Hataf (2003). The trend obtained by numerical simulations is, however, different; the results from the analyses show a decreasing trend from the beginning to the end. According to Clark (Clark 1998), such initial increase in the bearing capacity is due to the arching effect of the soil under the center of the ring footing. By comparing the results of the analyses, it can be said that the N_γ^* obtained by Benmebarek et al. (2012) and Kumar and Gosh (2005) underestimate the N_γ^* factor for all n ranges. The decreasing rate of N_γ^* with n is slow for the method of characteristics (Kumar and Gosh 2005), but N_γ^* variation obtained by Benmebarek et al. (2012) shows high rate with ring radii ratio. The N_γ^* values

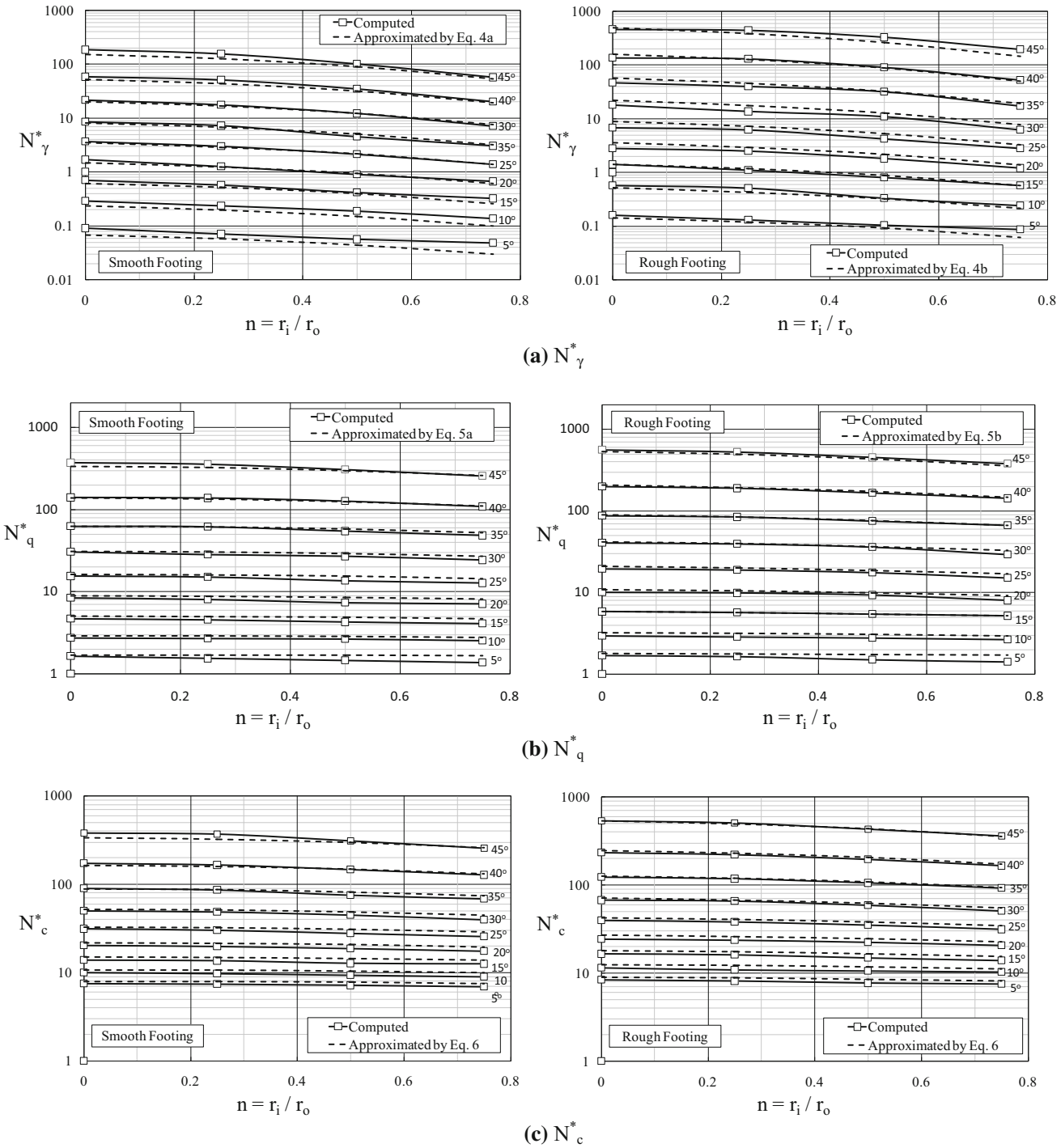

Fig. 4 Variation of bearing capacity factors versus the ring radii ratio for different values of friction angle for smooth and rough footings. **a** N^*_γ , **b** N^*_q, **c** N^*_c

obtained from the present simulations have more acceptable agreement with the experiment with the exception of $n = 0$.

In order to make the bearing capacity equation [Eq. (1)] more practical in the geotechnical engineering field, an attempt has been made to express the magnitudes of the bearing capacity factor N^*_γ in a mathematical form. Since the formulations of N^*_γ in the literature are usually expressed in terms of N^*_q, the same approach was followed here. Using mathematical functions and curve fitting technique by back analyses of data, a relationship between N^*_γ and N^*_q is suggested by the following expressions. For the smooth footing base, we suggest:

Table 1 Comparison of N_γ^* values from this study with results of other works for smooth and rough ring footings

ϕ (deg)	r_i/r_o	Smooth footing				Rough footing			
		Finite difference method			Method of characteristics	Finite difference method			Method of characteristics
		Present study	Zhao and Wang (2008)	Benmebarek et al. (2012)	Kumar and Gosh (2005)*	Present study	Zhao and Wang (2008)	Benmebarek et al. (2012)	Kumar and Gosh (2005)
10	0.25	0.23	0.13	–	0.18	0.51	0.73	–	0.25
	0.5	0.19	0.04	–	0.14	0.33	0.21	–	0.19
	0.75	0.14	–	–	0.07	0.24	–	–	0.1
20	0.25	1.3	0.86	0.86	1.2	2.5	3.84	1.75	1.77
	0.5	0.9	0.29	0.55	0.7	1.8	1.34	1.09	1.37
	0.75	0.7	–	0.3	0.4	1.2	–	0.6	0.78
30	0.25	7.2	4.69	5.14	6.3	13.6	18.1	12.9	11.67
	0.5	4.5	1.96	2.98	4.1	10.9	6.93	6.93	9.21
	0.75	3.0	–	1.5	1.9	6.2	–	3.43	5.35
40	0.25	50.9	–	40.2	39	129.6	–	123.4	103.88
	0.5	34.7	–	21.6	26	90.7	–	65.9	85.71
	0.75	20.1	–	9.78	11	52.1	–	26.7	51.86

* Values are derived from graphs

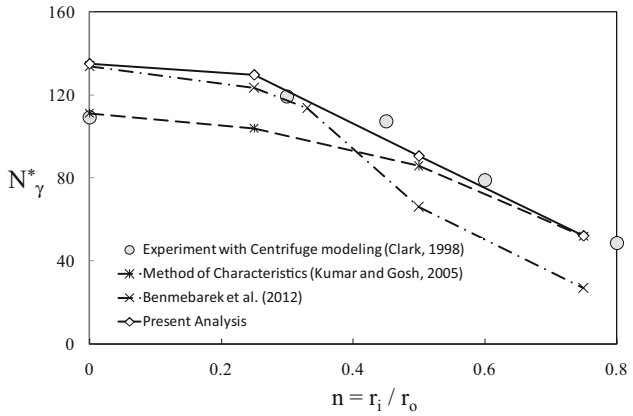

Fig. 5 Comparison of N_γ^* values obtained from the present study, centrifugal tests, and the analyses by others ($\phi = 40°$ is assumed)

$$N_\gamma^{*S} \approx 0.1(1.2 - n)(n + 3.8)N_q^{*S} \tan\phi \tag{3a}$$

and for a rough footing base, we have:

$$N_\gamma^{*R} \approx 0.2(1.2 - n)(n + 3.8)N_q^{*R} \tan\phi \tag{3b}$$

The superscripts S and R stand for smooth and rough footings, respectively. The value of N_q^* is discussed in the following section. The N_γ^* values from Eq. (3) are shown in Fig. 4a for comparison. Note that the formulas (3a) and (3b) predict the values of N_γ^* lower for $\phi = 5°$.

To examine Eq. (3), the expression is compared with the prediction of N_γ^* of a strip footing. It is expected that a ring footing with a big n close to one $(n \approx 1)$ behaves such as a strip footing, because plastic regions generated below the footing body are far enough and they do not interrupt each other. In this case, the third sentence of Eq. (1) can be rearranged in terms of $(r_o - r_i)$ in order to be comparable with strip footings by considering the corresponding sentence of Eq. (1). As a consequence, the equivalent factor for strip footing becomes: $N_{\gamma strip}^* = N_\gamma^*/(1 - n)$.

Figure 6 presents the variation of $N_{\gamma strip}^*$ value with the soil friction angle, which is estimated from Eq. (3a) by considering $n = 0.9$ as well as those introduced for strip footings (Terzaghi 1943; Vesic 1973; Hansen 1970; Meyerhof 1963; Martin 2005). As shown, there is generally good agreement between the prediction of $N_{\gamma strip}^*$ from the present analysis with those of the well-known formulations for strip footing, especially for $\phi > 20^o$.

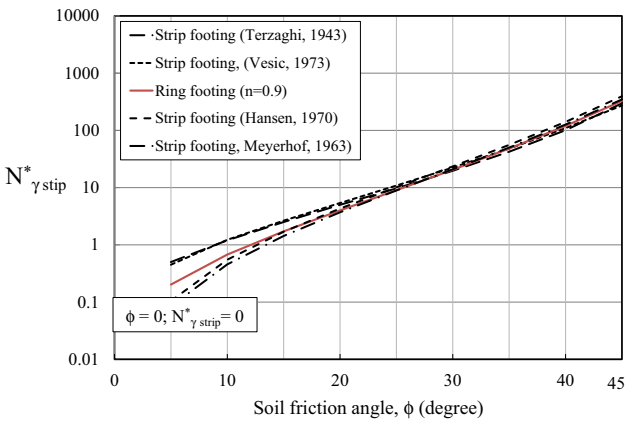

Fig. 6 Variation of N_γ^* value with the soil friction angle for a ring footing with $n = 0.9$ and for strip footings defined by various authors

4.2 Bearing Capacity Factor N_q^*

As mentioned before in the Introduction section, there is no study in the literature for N_q^* factor of ring footings. In order to evaluate the N_q^* factor obtained in this study, a comparison is provided here for circular footings with previous published works according to Table 2. It can be seen that all approaches give almost the same N_q^* value. The results of the present work satisfy the lower bounds presented by Kumar and Khatri (2011).

Similar to what was done for N_γ^*, mathematical expressions are proposed for the N_q^* factor in terms of soil friction angle and ring footing shape. For smooth footing, we obtain:

$$N_q^{*S} \approx \tan^2\left(45+\frac{\phi}{2}\right)e^{0.45(9-n^2)\tan\phi} \tag{4a}$$

and for rough footing, N_q^* is defined as follows:

$$N_q^{*R} \approx [1+0.3(2-n)\tan\phi]N_q^{*S} \tag{4b}$$

The predicted values from Eq. (4) are depicted in Fig. 4b. The expression generally coincides well over the values obtained from the present analysis.

A comparison between the prediction of N_q^* value of a ring footing with $n = 0.9$ [Eq. (4a)] and that of a strip footing for different friction angles is graphically shown in Fig. 7a. Although the N_q^* factor by Eq. (4a) is predicted slightly larger than that of the strip footing, a good match generally exists between the different approaches.

4.3 Bearing Capacity Factor N_c^*

A comparative study over N_c^* value from different methods mentioned above as well as the results of finite difference method performed by Erickson and Drescher (2002) is considered here for circular footing. The results are given in Table 3. It can be understood that the results of the present work and totally, the results from various methods match well with each other for both cases of smooth and rough footings. The exception corresponds to the approach proposed by Bolton and Lau (1993) in which the N_c^* value has the same value for smooth and rough footings.

It can be shown that, based on the Mohr stress circle, there is always a relationship between N_c^* and N_q^* factors by the following equation (Bolton and Lau 1993):

$$N_c^* = (N_q^* - 1)\cot\phi \tag{5}$$

This relationship holds true for both smooth and rough footings. The predicted values are shown in Fig. 4c that are acceptably coincident to the calculated values. N_c^* of a ring footing with $n = 0.9$ is compared with that of a strip footing. According to Fig. 7b, there is good agreement between the results.

Table 2 Comparison of N_q^* values from this study with results of other authors for smooth and rough circular footings

ϕ (deg)	Footing roughness	Finite difference method Present study	Method of characteristics			Lower bound finite element limit analysis Kumar and Khatri (2011)
			Martin (2004)	De Simone (1985)	Bolton and Lau (1993)	
5	Smooth	1.64	1.65	1.67	1.65	1.64
	Rough	1.70	1.71	1.71		1.70
10	Smooth	2.75	2.76	2.74	2.8	2.72
	Rough	2.95	2.96	3.01		2.94
15	Smooth	4.7	4.72	4.62	4.7	4.62
	Rough	5.5	5.25	5.23		5.20
20	Smooth	8.4	8.31	8.24	8.3	8.05
	Rough	10.1	9.62	9.73		9.45
25	Smooth	15.5	15.23	14.92	15.2	14.55
	Rough	19.6	18.40	18.34		17.87
30	Smooth	30.5	29.46	28.52	29.2	28.20
	Rough	40.8	37.21	36.55		36.50
35	Smooth	62.5	6.11	59.22	61	58.04
	Rough	87.6	80.81	79.11		79.75
40	Smooth	139.8	139.20	131.75	140	130.17
	Rough	198.8	192.70	185.98		189.19
45	Smooth	371	359.10	336.47	359	325.85
	Rough	560	520.60	501.88		502.74

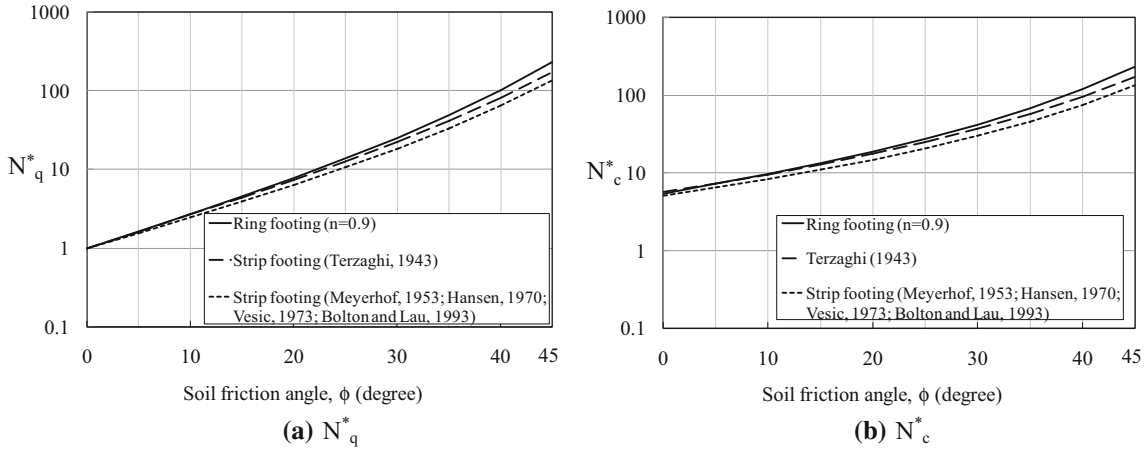

Fig. 7 Variation of N_q^* and N_c^* with the soil friction angle for a ring footing with $n = 0.9$ and for strip footings defined by other authors. **a** N_q^*. **b** N_c^*

Table 3 N_c^* from this study and other authors for smooth and rough circular footings

ϕ (deg)	Footing roughness	Finite difference method		Method of characteristics		Lower bound finite element limit analysis
		Present study	Erickson and Drescher (2002)	Martin (2004)	Bolton and Lau (1993)	Kumar and Khatri (2011)
0	Smooth	5.7	–	6.69	–	5.61
	Rough	6.1	–	6.05		6.01
5	Smooth	7.5	–	7.43	7.43	7.31
	Rough	8.4	–	8.06		8.00
10	Smooth	10	–	9.99	10.21	9.78
	Rough	11.5	–	11.09		10.99
15	Smooth	13.9	–	13.87	13.81	13.51
	Rough	16.5	–	15.84		15.66
20	Smooth	20.3	19.5	20.07	20.06	19.38
	Rough	24.2	22.3	23.67		23.22
25	Smooth	31.2	–	30.52	30.45	29.06
	Rough	39.5	–	37.31		36.17
30	Smooth	50	–	49.29	49.36	47.10
	Rough	67	–	62.70		61.48
35	Smooth	90	84	85.88	85.69	81.47
	Rough	122.5	108	113.99		112.47
40	Smooth	172.5	161	164.82	165.65	153.94
	Rough	233	186	228.62		224.27
45	Smooth	380	320	358.81	358	324.85
	Rough	535	380	520.31		501.74

5 Examination of the Bearing Capacity Equation

In the derivation of bearing capacity equation [Eq. (1)], it is assumed that the contributions of soil weight, cohesion, and surcharge are superposed. This enables the formula to be approximate because plasticity solutions do not satisfy the superposition principle, which is valid in the linear elasticity problems. For strip and circular footings, it has been shown that using such superposition in the bearing capacity problems gives conservative estimates (Hansen 1970; Bolton and Lau 1993; Michalowski 1997). In order to investigate the conservatism of Eq. (1) for ring footings, several examples are considered here. The bearing capacity of six series of ring footings with $D_o = 3,6$ m was computed by a direct numerical simulation using FDM as well as using Eq. (1), which is based on the superposition

Table 4 Properties of the soil and the surcharge used in the examination of the bearing capacity problems

Series 1	Series 2	Series 3	Series 4	Series 5	Series 6
$D_0 = 6$ m			$D_0 = 3$ m		
$\gamma = 18$ kN/m^3	$\gamma = 18$ kN/m^3	$\gamma = 18$ kN/m^3	$\gamma = 17$ kN/m^3	$\gamma = 17$ kN/m^3	$\gamma = 17$ kN/m^3
$\phi = 35°$	$\phi = 35°$	$\phi = 35°$	$\phi = 25°$	$\phi = 25°$	$\phi = 25°$
$q_0 = 200$ kPa	$q_0 = 0$ kPa	$q_0 = 200$ kPa	$q_0 = 100$ kPa	$q_0 = 0$ kPa	$q_0 = 100$ kPa
$c = 50$ kPa	$c = 50$ kPa	$c = 0$	$c = 30$ kPa	$c = 30$ kPa	$c = 0$

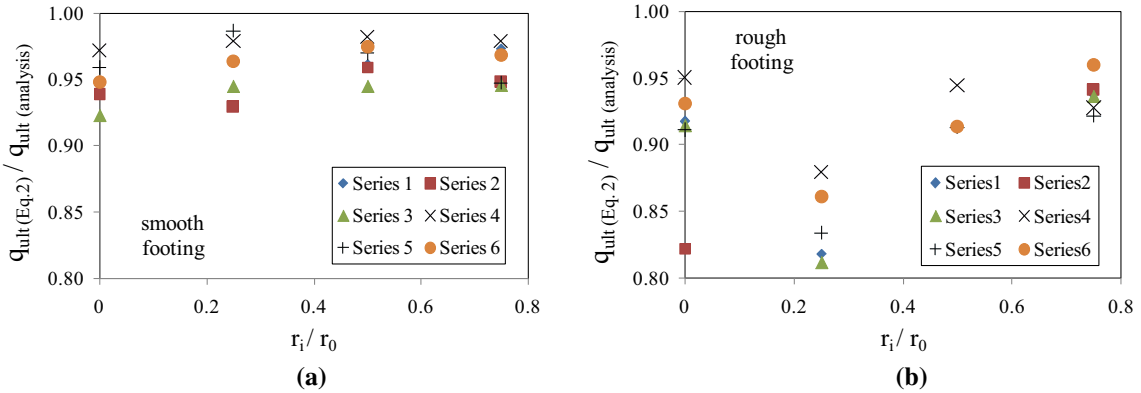

Fig. 8 Variation of the bearing capacity ratio from prediction [Eq. (1)] and direct plastic analysis with ring radii ratio: **a** smooth footings; **b** rough footings for six series according to Table 4

principle. The soil properties and the surcharge used in this examination are presented in Table 4.

The comparison of the results is achieved by a graphical presentation shown in Fig. 8 as the variation of the bearing capacity ratio calculated by using Eq. (1) and direct numerical analysis versus the ring radii ratio. Globally, it can be determined that the bearing capacity ratio from all the series have been obtained less than unity, which confirms the conservativeness of Eq. (1).

The degree of noncoincidence between these approaches differs for smooth and rough footing cases. According to Fig. 8a, the maximum difference between these approaches is about 5–10 % for smooth footings. For the rough footings, in accordance with Fig. 5b, the same range of error exists, but it becomes higher at $n = 0.25$. This pertains to the fact that by using the direct analysis approach, the bearing capacity shows a slight increase at $n = 0.25$ with respect to $n = 0$ and 0.5. This occurrence implies that if surcharge or soil cohesion is taken into consideration in conjunction with the soil weight, it would be possible to reach the arching mechanism in the numerical analyses. In this condition, the bearing capacity of rough ring footings never reduces with the increase in ring radii ratio, but the bearing capacity can be obtained higher with respect to circular footing case. The same trend can be found in the results of numerical analyses of ring footings performed by Boushehrian and Hataf (Boushehrian and Hataf 2003) and Choobbasti et al. (2010) using FEM. As already mentioned in "Introduction" section, investigation on the arching mechanism in the ring footings is out of the scope of the present work, which requires a more detailed and elaborate study on the numerical modeling.

6 Conclusion

In this paper, the bearing capacity of ring footings was investigated by numerical simulations using the finite difference method and the factors defined in the classical Terzaghi's bearing capacity equation were determined. The computations were performed by considering the effect of footing roughness. According to the results, the factors N_γ^*, N_q^*, and N_c^* altogether are influenced by the ring geometry which is defined as inner to outer ring radii ratio as well as the footing roughness. As the ring radii ratio increases, i.e., the ring becomes narrower and the value of the factors decreases. Such decreasing effect is more sensible for the N_γ^* factor. The footing roughness causes the bearing capacity to increase. Based on the numerical results of the present work, mathematical expressions were introduced for the bearing capacity factors so that the results are more practical for geotechnical engineers.

By comparing the results of the present work with those of centrifugal tests, it was shown that there is an

acceptable agreement for the value as well as the decreasing trend of N_γ^* versus the ring radii ratio. The N_q^* and N_c^* factors in the case of circular footing were also compared with available data in the literature which shows good agreement.

Finally, some examples were solved in order to estimate the bearing capacity of ring footings by using the proposed bearing capacity equation. Knowing that the bearing capacity equation is the result of the superposition of different plastic conditions, it was shown, by these examples, that the proposed solution for ring footings gives smaller and conservative values with respect to a complete and rigorous plastic solution. Consequently, the bearing capacity equation and the mathematical expressions introduced in the paper can be applied in practice with desired safety.

Acknowledgments The author would like to express his appreciation to the Research Deputy of Ferdowsi University of Mashhad for supporting the present research by Grant No. 26983-31/02/92.

Appendix 1

In this appendix, an attempt is made to estimate the peak internal friction of the soil, which is mobilized under the footings corresponding to the ultimate bearing capacity. This is achieved by assuming that a triaxial stress condition under the footings exists and the ultimate bearing capacity has the role of the major principal stress induced in the soil.

Several triaxial compression tests were conducted on silica sand with a wide range of confining pressure $p' = 25$–2500 kPa. The results reported by Clark (Clark 1998) indicate that there is a linear relationship between the peak friction angle (ϕ_{peak}) and logarithm of stress level. The following expression can be derived:

$$\phi_{\text{peak}} = 49 - 5\log\left(\frac{p'}{25}\right) \tag{6}$$

The mean confining pressure (p') in the soil under the footing base for the triaxial condition is regarded as:

$$p' = \frac{\sigma_v' + 2\sigma_h'}{3} \tag{7}$$

where σ_v' and σ_h' are considered as the mean vertical and horizontal stress components in the soil below the ring footing. σ_v' can be estimated as the applied vertical pressure over the footing and σ_h' can be obtained by the lateral coefficient in the active condition (K_a) in the following way:

$$\frac{\sigma_h'}{\sigma_v'} = K_a = \tan^2\left(45 - \frac{\phi}{2}\right) \tag{8}$$

Table 5 Results from back-calculation of bearing capacity of ring footings

n	q_{ult} (kPa)	p' (kPa)	ϕ_{peak} (deg)
0	3900	1875	39.6
0.3	4250	2050	39.4
0.45	3700	1780	39.7
0.6	2700	1280	40.5
0.8	1600	750	41.5

Since the bearing capacity (q_{ult}) of ring footings was reported as the maximum applied vertical pressure over the footings, it is assumed that $\phi = \phi_{\text{peak}}$ and $\sigma_v' = q_{\text{ult}}$. The mean confining pressure can be rewritten in the following form:

$$p' = \left(\frac{1 + 2K_a}{3}\right) q_{\text{ult}} \tag{9}$$

By considering Eqs. (6) and (9) and following several successive calculations for the bearing capacity of every ring footing, the following results, according to Table 5, are obtained.

References

Benmebarek S, Remadna MS, Benmebarek N, Belounar L (2012) Numerical evaluation of bearing capacity factor N_g of ring footings. Comput Geotech 44:132–138

Bolton MD, Lau CK (1993) Vertical bearing capacity factors for circular and strip footings on Mohr–Coulomb soil. Can Geotech J 30:1024–1033

Boushehrian JH, Hataf N (2003) Experimental and numerical investigation of the bearing capacity of model circular and ring footings on reinforced sand. Geotext Geomembr 21:241–256

Choobbasti AJ, Hesami S, Najafi A, Pirzadeh S, Farrokhzad F, Zahmatkesh A (2010) Numerical evaluation of bearing capacity and settlement of ring footing, case study of Kazeroon cooling towers. Int J Res Rev Appl Sci 4:263–271

Clark JI (1998) The settlement and bearing capacity of very large foundations on strong soils: 1996 R.M. Hardy keynote address. Can Geotech J 35:131–145

De Beer EE (1965) Bearing capacity and settlement of shallow foundations on sand. In: Bearing capacity and settlement of foundation symposium. Duke University, Durham, pp 15–34

De Simone P (1985) Bearing capacity of a circular footing on a Coulomb medium. In: Proceedings of the 5th international conference on numerical methods in geomechanics, Nagoya, Japan, vol 2, pp 829–836

Erickson HL, Drescher A (2002) Bearing capacity of circular footings. J Geotech Geoenviron Eng 128:38–43

Haghbin M, Ghazavi M (2013) Bearing capacity of footings on pile-stabilized slopes. Iran J Sci Technol Trans B Eng 37:257–269

Hansen JB (1970) A revised and extended formula for bearing capacity. Danish Geotechnical Institute 28:5–11

Hataf N, Razavi MR (2003) Behavior of ring footing on sand. Iran J Sci Technol Trans B Eng 27:47–56

Houlsby GT (1982) Theoretical analysis of the fall cone test. Géotechnique 32:111–118

Keshavarz A, Jahanandish M, Ghahramani A (2011) Seismic bearing capacity analysis of reinforced soils by the method of stress characteristics. Iran J Sci Technol Trans B Eng 35:185–197

Kumar J, Gosh P (2005) Bearing capacity factor N_g for ring footings using the method of characteristics. Can Geotech J 42:1474–1484

Kumar J, Khatri VN (2011) Bearing capacity factors of circular foundations for a general c–f soil using lower bound finite elements limit analysis. Int J Numer Anal Methods Geomech 35:393–405

Majidi AR, Mirghasemi AA (2008) Seismic 3D bearing capacity analysis of shallow foundations. Iran J Sci Technol Trans B Eng 32(2):175–179

Martin CM (2004) User guide for ABC–analysis of bearing capacity, version 1.0. Software and documentation available online from www.civil.eng.ox.ac.uk

Martin CM (2005) Exact bearing capacity calculations using the method of characteristics. In: 11th international conference IACMAG. Turin, pp 441–450

Meyerhof GG (1951) The ultimate bearing capacity of foundations. Géotechnique 2:301–332

Meyerhof GG (1963) Some recent research on the bearing capacity of foundations. Can Geotech J 1:16–26

Michalowski RL (1997) An estimate of the influence of soil weight on bearing capacity using limit analysis. Soils Found 37:57–64

Ohri ML, Purhit DGM, Dubey ML (1997) Behavior of ring footings on dune sand overlaying dense sand. In: Proceedings of international conference of civil engineers. Tehran, Iran

Rostami V, Ghazavi M (2015) Analytical solution for calculation of bearing capacity of shallow foundations on geogrid-reinforced sand slope. Iran J Sci Technol Trans B Eng 39:167–182

Taylor RN (1995) Geotechnical centrifuge technology. Taylor and Francis, Glasgow

Terzaghi K (1943) Theoretical soil mechanics. Wiley, New York

Vesic AA (1973) Analysis of ultimate loads of shallow foundations. J Soil Mech Found Eng ASCE 99:45–73

Zhao L, Wang JH (2008) Veritcal bearing capacity for ring footings. Comput Geotech 35:292–304

Zhu F, Clark JI, Phillips R, Kosar KM (1996) Centrifuge modeling of ring footings. In: Proceedings of the 49th Canadian geotechnical conference. St. John's Nfld 1996, pp 539–546